frontiers in Earth Science

REVIEW
published: 31 July 2020
doi: 10.3389/feart.2020.00316

Mercury Deposition, Climate Change and Anthropogenic Activities: A Review

Feng Li[1], Chunmei Ma[1] and Pingjiu Zhang[2]*

[1] School of Geography and Ocean Science, Nanjing University, Nanjing, China, [2] School of Geography and Tourism, Anhui Normal University, Wuhu, China

As a toxic and harmful global pollutant, mercury enters the environment through natural sources, and human activities. Based on large numbers of previous studies, this paper summarized the characteristics of mercury deposition and the impacts of climate change and human activities on mercury deposition from a global perspective. The results indicated that global mercury deposition changed synchronously, with more accumulation during the glacial period and less accumulation during the interglacial period. Mercury deposition fluctuated greatly during the Early Holocene but was stable and low during the Mid-Holocene. During the Late Holocene, mercury deposition reached the highest value. An increase in precipitation promotes a rise in forest litterfall Hg deposition. Nevertheless, there is a paucity of research on the mechanisms of mercury deposition affected by long-term humidity changes. Mercury accumulation was relatively low before the Industrial Revolution ca. 1840, while after industrialization, intensive industrial activities produced large amounts of anthropogenic mercury emissions and the accumulation increased rapidly. Since the 1970s, the center of global mercury production has gradually shifted from Europe and North America to Asia. On the scale of hundreds of thousands of years, mercury accumulation was greater in cold periods and less in warm periods, reflecting exogenous dust inputs. On millennial timescales, the correspondence between mercury deposition and temperature is less significant, as the former is more closely related to volcanic eruption and human activities. However, there remains significant uncertainties such as non-uniform distribution of research sites, lack of mercury deposition reconstruction with a long timescale and sub-century resolution, and the unclear relationship between precipitation change and mercury accumulation.

Keywords: mercury deposition, site distribution, climate change, anthropogenic activities, industrialization

OPEN ACCESS

Edited by:
Liangcheng Tan,
Chinese Academy of Sciences, China

Reviewed by:
Guanghui Dong,
Lanzhou University, China
Ruoyu Sun,
Tianjin University, China

****Correspondence:***
Chunmei Ma
chunmeima@nju.edu.cn

Specialty section:
This article was submitted to Quaternary Science, Geomorphology and Paleoenvironment, a section of the journal Frontiers in Earth Science

Received: *21 January 2020*
Accepted: *03 July 2020*
Published: *31 July 2020*

Citation:
Li F, Ma C and Zhang P (2020) Mercury Deposition, Climate Change and Anthropogenic Activities: A Review. Front. Earth Sci. 8:316. doi: 10.3389/feart.2020.00316

INTRODUCTION

As a toxic and harmful global pollutant, mercury enters the environment through natural sources (volcanic eruptions, oceans, soil, and forests, etc.), and human activities (fossil fuel combustion; gold, silver, and mercury mining; non-ferrous metal smelting; etc.; Tang et al., 2012; Guédron et al., 2018; Obrist et al., 2018; Pratte et al., 2018). Mercury in the atmosphere includes particulate mercury and gaseous mercury. Particulate mercury includes Hg(0) and $HgCl_2$, among others, which are adsorbed on the surface of particles or combined with particles; gaseous mercury mainly

exists in the form of Hg(O) (Wang, 2011). Due to its high volatility, low chemical activity, and low solubility, mercury is characterized by a long atmospheric life (0.5–2 years), and long-distance transport (Roos-Barraclough et al., 2002). Furthermore, there are a few other volatile mercury compounds, including $HgBr_2$, $HgCl_2$, and $Hg(OH)_2$, that are easily soluble in water and reduced to Hg(0), referred to as reactive gaseous mercury (RGM; Wang, 2011). Mercury under long-distance transportation can enter natural archives, including peatlands, lacustrine deposits, ice cores, coastal salt marsh sediments, and marginal pelagic sediments, through dry and wet deposition (Schuster et al., 2002; Tang et al., 2012; Donovan et al., 2013; Krabbenhoft and Sunderland, 2013; Guédron et al., 2018; Kim et al., 2019). These characteristics of mercury accumulation in natural archives can, to some extent, reflect the process of atmospheric mercury deposition during historical periods, and the deposition rate may be subject to factors such as climate change, geological conditions, volcanic eruptions, and human activities in the natural environment (Biester et al., 2007; Guédron et al., 2019).

In recent years, there have been many studies reconstructing atmospheric mercury deposition during historical periods using the natural archives. These studies focused mainly on the Northern Hemisphere, whereas studies in the Southern Hemisphere were limited to Chile (Biester et al., 2002, 2003; Hermanns and Biester, 2013a,b; Daga et al., 2016; Guédron et al., 2019), Brazil (Peìrez-Rodrìguez et al., 2015; De Lacerda et al., 2017), and Peru of South America (Cooke et al., 2009; Beal et al., 2014). In the Northern Hemisphere, European countries, represented by Switzerland (Roos-Barraclough et al., 2002; Roos-Barraclough and Shotyk, 2003; Zaccone et al., 2008; Thevenon et al., 2011), Spain (Martínez-Cortizas et al., 1999, 2012; Gallego et al., 2013; Serrano et al., 2013; Corella et al., 2017), Denmark (Shotyk et al., 2003), Greenland (Shotyk et al., 2003; Zheng, 2015; Pérez-Rodríguez et al., 2017), Scotland (Farmer et al., 2009; Küttner et al., 2014), Norway (Steinnes and Sjøbakk, 2005; Drevnick et al., 2012), and Sweden (Bindler et al., 2004), were studied mostly in terms of mercury deposition, followed by North America, represented by Canada (Givelet et al., 2004; Sunderland et al., 2008; Zdanowicz et al., 2015, 2016; Wiklund et al., 2017; Korosi et al., 2018; Štrok et al., 2019), and the United States (Benoit et al., 1998; Schuster et al., 2002; Arnason and Fletcher, 2003; Conaway et al., 2004; Gray et al., 2005; Roos-Barraclough et al., 2006; Donovan et al., 2013; Megaritis et al., 2014; Kurz et al., 2019). In contrast, there have been fewer studies on mercury deposition in China, with the research areas mainly distributed in the Shennongjia Dajiu Lake Basin (Li et al., 2016, 2017), the Greater Khingan Range (Bao et al., 2016), the Lesser Khingan Range (Xu et al., 2010; Tang et al., 2012), the Tibetan Plateau (Wang et al., 2010; Yang et al., 2010; Huang et al., 2013), and the South China Sea (Xu et al., 2010; Liu et al., 2012). In turn, there have numerous time series analyses that document changes in mercury deposition on 10^3 to 10^1 timescales that evaluate the impact of climate change and human activities on mercury deposition. However, these studies were almost always limited to a certain place or a certain area and explained only the mercury accumulation in a certain area. We are unaware of previous reviews of mercury deposition on a longer timescale from a global perspective. The authors hoped to find similarities and differences between different regions by analyzing and summarizing historical mercury deposition data at a global scale, and explored the relationship between mercury deposition and climate change and human activities.

This paper identified and analyzed relevant studies on atmospheric mercury deposition regarding climate change and human activities from a global perspective, discussing the prospects for future research. The global mercury deposition history reflected the global climate change and regional human activities during historical periods. Our work is conducive to the systematic understanding of mercury deposition and its influencing factors. On this basis, new methods and perspectives can be developed to conduct more in depth research.

DATA SOURCES

The data used in this study were mainly based on peer-reviewed papers and the data for Dajiu Lake Basin from our research group. The authors searched for documents in Elsevier SDOL, Nature, Science, Google Scholar, and the CNKI database, among others, using keywords such as "mercury deposition/mercury accumulation," "climate change," and "anthropogenic activities/human activities." Following the principles of a uniform spatial distribution and an extensive timescale, 36 sets of mercury deposition data from 60 papers were selected, covering the history of atmospheric mercury deposition on six continents (Asia, Europe, Africa, North America, South America, and Antarctica) recorded by natural archives (fen peat, lacustrine deposits, ice cores, and marine deposits, etc.) from 670 ka BP to now, as shown in **Table 1**.

According to the global studies on atmospheric mercury deposition, the authors found that the site distribution of global mercury deposition studies was characterized by an overall pattern of "more in the north and fewer in the south"; that is, the research areas were mostly distributed in the Northern Hemisphere, such as Europe (including Belgium, the Czech Republic, Denmark, Greenland, Ireland, Norway, Scotland, Spain, Sweden, and Switzerland), North America (including the United States and Canada), and China (including the Northeast Hani, Shennongjia Dajiu Lake Basin, Greater Khingan Range, Lesser Khingan Range, Sichuan Hongyuan, Huguangyan Maar Lake, Chao Lake, Tibetan Plateau, Xinjiang Mount Tianshan, East China Sea, Yellow Sea, and South China Sea), while in the Southern Hemisphere, the areas were distributed only in South America (including Chile, Peru, Brazil, and Bolivia), Africa (including the Berg River of South Africa and Lake Tanganyika in East Africa), and some parts of Antarctica, as shown in **Figure 1**.

RESULTS AND DISCUSSION

Regional Comparison of Global Mercury Deposition

At the global scale, atmospheric mercury deposition is closely related to climate variability (such as temperature and humidity changes) and human activities (such as mining, metal smelting,

TABLE 1 | Information of global mercury deposition research spots.

Number	Study site	Region	Location	Altitude/m	Materials dated	Depth/m	Dating methods	Age range	Selected references
a1	The Upper Fremont Glacier	Wyoming, United States	44°20′02″ N 111°36′49″ W	4100	Ice core	160	Isotope and chemical dating	1720–1993 AD	Schuster et al., 2002
a2	San Francisco Bay	United States	37°40′00″ N 122°25′00″ W	/	Coastal salt marsh	1.6	^{137}Cs, ^{210}Pb	1850–2000 AD	Donovan et al., 2013
a3	Southern Baffifin Island	Arctic Canada	63°57′53″ N 68°15′42″ W	1825	Firn	22.7	δ^{18}O	1970–2010 AD	Zdanowicz et al., 2015
a4	The Bay of Fundy	Canada	45°12′36″ N 66°54′12″ W	/	Peat bogs, Lake sediments, Coastal salt marsh	/	^{137}Cs, ^{210}Pb	1800–2000 AD	Sunderland et al., 2008
a5	Lake Ontario	Canada	49°48′00″ N 93°48′00″ W	/	Lake sediments	/	^{137}Cs, ^{210}Pb	1850–2000 AD	Wiklund et al., 2017
a6	Ellesmere Island	The Canadian High Arctic Archipelago	78°43′00″ N 74°27′00″ W	323	Lake sediments	12.1	^{137}Cs, ^{210}Pb	1850–2000AD	Korosi et al., 2018
a7	Caribou Bog	Central Maine, United States	44°58′97″ N 68°48′35″ W	80	Peat bogs	5	^{210}Pb, ^{14}C	8000 BC–2000 AD	Roos-Barraclough et al., 2006
a8	Lost Lake	Wyoming, United States	43°46′55″ N 110°06′00″ W	2889	Lake sediments	21	^{137}Cs, ^{210}Pb	1350–2000 AD	Kurz et al., 2019
a9	Oyster Point	California, United States	45°25′28″ N 111°20′28″ W	/	Coastal salt marsh	3	^{14}C	1700–2000 AD	Conaway et al., 2004
a10	Arlberg Bog	Minnesota, United States	46°56′00″ N 92°41′00″ W	/	Peat bogs	0.6	^{137}Cs, ^{210}Pb	1700–2000 AD	Benoit et al., 1998
a11	Narraguinnep Reservoir	Colorado, United States	40°31′26″ N 106°58′43″ W	2035	Lake sediments	10	^{137}Cs	1950–2000 AD	Gray et al., 2005
a12	Patroon Reservoir	New York, United States	42°41′05″ N 73°47′21″ W	/	Lake sediments	3	/	1955–2000 AD	Arnason and Fletcher, 2003
b1	Etang de la Gruère	Swiss Jura Mountains	47°15′34″ N 07°03′51″ E	1005	Peat bogs	6.5	^{210}Pb, ^{241}Am, ^{14}C	12500 BC–2000 AD	Roos-Barraclough et al., 2002
b2	Franches Montagnes	Swiss Jura Mountains	47°14′23″ N 07°02′57″ E	1020	Peat bogs	0.8	^{210}Pb, ^{14}C	1200 BC–2000 AD	Roos-Barraclough and Shotyk, 2003
b3	Lake Lucerne	Central Switzerland	46°13′25″ N 07°40′28″ E	2661	Lake sediments	1.2	^{14}C	14315 BC–2000 AD	Thevenon et al., 2011
b4	Roñanzas Bog	Asturias, Spain	43°20′13″ N 04°51′01″ W	/	Peat bogs	2	/	6000 BC–2000 AD	Gallego et al., 2013
b5	Galicia	Northwest Spain	43°32′00″ N 07°34′00″ W	/	Peat bogs	2.5	^{14}C	2635 BC–1995 AD	Martínez-Cortizas et al., 1999
b6	Lake Montcortès	Pyrenees, Spain	42°19′00″ N 00°19′00″ E	1031	Lake sediments	1.1	^{210}Pb, ^{14}C	1386–2010 AD	Corella et al., 2017
b7	Chao de Lamoso bog	Xistral Mountains, northwest Spian	43°14′35″ N 09°05′45″ W	1039	Peat bogs	1	^{210}Pb	1825–2000 AD	Martínez-Cortizas et al., 2012
b8	Portlligat Bay	Iberian Peninsula	42°17′32″ N 03°17′28″ E	/	Coastal salt marsh	5	^{14}C	2315 BC–2000 AD	Serrano et al., 2013
b9	Storelung Mose	Denmark	55°15′23″ N 10°15′22″ E	/	Peat bogs	1	^{14}C	2000 BC–2000 AD	Shotyk et al., 2003

(Continued)

TABLE 1 | Continued

Number	Study site	Region	Location	Altitude/m	Materials dated	Depth/m	Dating methods	Age range	Selected references
b10	Sandhavn	Southern Greenland	59°59′54″ N 44°46′36″ W	/	Peat bogs	0.4	^{210}Pb, ^{14}C	1270–2000 AD	Pérez-Rodríguez et al., 2017
b11	Raeburn Flow	Scotland, United Kingdom	55°02′04″ N 03°06′27″ W	/	Peat bogs	3.6	^{210}Pb, ^{14}C	1385 BC–2005 AD	Küttner et al., 2014
b12	Six ombrotrophic bogs	Norway	58°–69° N 04°–12° E	/	Peat bogs	1	^{210}Pb, ^{14}C	2000 BC–2000 AD	Steinnes and Sjøbakk, 2005
b13	Svalbard	Norwegian Arctic	80°03′05″ N 17°37′26″ E	/	Lake sediments	/	^{210}Pb	1800–1995 AD	Drevnick et al., 2012
b14	Store Mosse	South-central Sweden	57°15′00″ N 13°55′00″ E	/	Peat bogs	0.4	^{137}Cs, ^{210}Pb	1860–2000 AD	Bindler et al., 2004
b15	Marano and Grado Lagoon	Northern Adriatic Sea	40°12′–45°53′ N 12°13′–19°34′ E	/	Coastal salt marsh	1.1	^{137}Cs, ^{210}Pb	1650–2000 AD	Covelli et al., 2012
b16	Misten peat bog	Eastern Belgium	50°38′28″ N 03°11′17″ E	/	Peat bogs	1	^{210}Pb, ^{14}C	431–2011 AD	Allan et al., 2013
b17	Brdy Hills	The Czech Republic	49°42′42″ N 13°52′30″ E	/	Peat bogs	0.38	^{210}Pb	1807–2003 AD	Ettler et al., 2008
b18	Multiple lakes	Across England	50°–55° N 04° W–02° E	3–244	Lake sediments	1.5	^{137}Cs, ^{210}Pb, ^{241}Am	1850–2010 AD	Yang H. D. et al., 2016
c1	Tanghongling	Heilongjiang Province, northeast China	46°42′–48°40′ N 129°05′–129°55′ E	/	Peat bogs	1.05	^{210}Pb, ^{14}C	4480 BC–2000 AD	Tang et al., 2012
c2	Dajiu Lake Basin	Hubei Province, China	31°29′27″ N 109°59′45″ E	1760	Peat bogs	2.97	^{14}C	14141 BC–2004 AD	Li et al., 2017
c3	Motianling mountain	Western Great Hinggan Mountains, China	46°39′–47°39′ N 119°28′–121°23′ E	1200	Peat bogs	0.78	^{137}Cs, ^{210}Pb	1820–2005 AD	Bao et al., 2016
c4	Tibetan Plateau	Southwest China	28°41′–37°17′ N 85°23′–100°16′ E	2813–4652	Lake sediments	0.4	^{137}Cs, ^{210}Pb, ^{241}Am, ^{226}Ra	1830–2010 AD	Yang et al., 2010
c5	Qinghai Lake	Northeast Tibetan Plateau, China	36°24′00″ N 100°09′00″ E	/	Lake sediments	0.205	^{137}Cs, ^{210}Pb, ^{241}Am, ^{226}Ra	1860–2000 AD	Wang et al., 2010
c6	Guangjin Islan	South China Sea	16°27′07″ N 111°42′05″ E	/	Eggshells	1.05	^{210}Pb, ^{14}C	1280–2000 AD	Xu et al., 2010
c7	Xisha Islands	South China Sea	15°47′–17°08′ N 110°10′–112°55′ E	/	Coral sand	0.95	^{210}Pb, ^{14}C	1300–2000 AD	Liu et al., 2012
c8	Lake Sayram	Xinjiang Province, China	44°30′–44°42′ N 81°05′–81°15′ E	2072	Lake sediments	0.3	^{210}Pb	1810–2010 AD	Zeng et al., 2014
c9	Hani peat bog	Jilin Province, China	42°12′50″ N 126°31′05″ E	882–900	Peat bogs	9	^{14}C	11927 BC–2010 AD	Xiao, 2017
c10	Okinawa Trough	East China Sea	27°29′50″ N 126°41′16″ E	/	Marginal pelagic sediments	4.95	^{14}C	17990 BC–2010 AD	Lim et al., 2017

(Continued)

TABLE 1 | Continued

Number	Study site	Region	Location	Altitude/m	Materials dated	Depth/m	Dating methods	Age range	Selected references
c11	East China Sea	China	26°–32° N 120°–126° E	/	Marginal pelagic sediments	1.4	^{137}Cs, ^{210}Pb	1913–2015 AD	Zhang R. et al., 2018
c12	Shanghai	China	31°26′17″ N 121°23′02″ E	/	Lake sediments	0.35	^{137}Cs, ^{210}Pb	1750–2010 AD	Yang J. et al., 2016
c13	Chao Lake	Anhui Province, China	31°25′–31°43′ N 117°16′–117°51′ E	/	Lake sediments	0.3	^{210}Pb	1890–2009 AD	Zhang H. X. et al., 2018
c14	Hongyuan	Sichuan Province, China	32°46′46″ N 102°30′58″ E	3510	Peat bogs	0.25	^{210}Pb	1850–2006 AD	Shi et al., 2011
c15	Huguangyan Maar Lake	Guangdong Province, China	21°09′00″ N 110°17′00″ E	/	Lake sediments	0.94	^{137}Cs, ^{14}C	766–2005 AD	Han, 2018
c16	Huguangyan Maar Lake	Guangdong Province, China	21°09′00″ N 110°17′00″ E	/	Lake sediments	1.175	^{137}Cs, ^{210}Pb, ^{14}C	1350–2004 AD	Zeng et al., 2017
d1	Lake Titicaca region	Bolivia	15°50′–16°13′ S 68°03′–68°17′ W	3760–4040	Peat bogs	1.63	^{14}C	11430 BC–2014 AD	Guédron et al., 2018
d2	Lake Chungará	Chile	18°15′07″ S 69°09′47″ W	4520	Lake sediments	1.46	^{137}Cs, ^{210}Pb	686 BC–2014 AD	Guédron et al., 2019
d3	Lake Hambre	Patagonia, Chile	53°36′13″ S 70°57′08″ W	80	Lake sediments	13.94	^{14}C	14722 BC–2008 AD	Hermanns and Biester, 2013a
d4	The Gran Campo bog	Magellanic Moorlands, Chile	52°47′26″ S 72°56′37″ W	/	Peat bogs	1.5	^{210}Pb, ^{14}C	466 BC–1995 AD	Biester et al., 2002
d5	Lake Futalaufquen	Patagonia, Chile	42°49′00″ S 71°43′00″ W	518	Lake sediments	0.79	^{137}Cs	400–2000 AD	Daga et al., 2016
d6	Pinheiro Mire	Minas Gerais, Brazil	18°03′44″ S 43°39′42″ W	1230–1270	Peat bogs	2.2	^{14}C	54990 BC–2010 AD	Peìrez-Rodrïguez et al., 2015
d7	Yanacocha	Southeast Peru	13°56′42″ S 70°52′30″ W	4910	Lake sediments	3.33	^{210}Pb, ^{14}C	10290 BC–2010 AD	Beal et al., 2014
d8	Huancavelica	Central Peru	14°51′27″ S 75°24′38″ W	/	Lake sediments	/	^{210}Pb, ^{14}C	2800 BC–2000 AD	Cooke et al., 2009
e1	Berg River	South Africa	32°47′26″ S 18°12′05″ E	/	Coastal salt marsh	0.3	^{210}Pb	1900–2007 AD	Kading et al., 2009
e2	Lake Tanganyika	East Africa	04°40′–06°34′ S 29°37′–29°59′ W	/	Lake sediments	0.28	^{210}Pb, ^{14}C	1600–2000 AD	Conaway et al., 2012
f1	King George Island	Western Antarctica	62°11′57″ S 59°58′48″ W	/	Seal hairs	0.425	^{137}Cs, ^{14}C	18–2002 AD	Sun et al., 2006
f2	Adélie Basin	Southern Antarctica	66°12′53″ S 140°26′17″ E	/	Diatom ooze sediments	170	Diatom fossils	6600 BC–2000 AD	Zaferani et al., 2018
f3	Dome C	Antarctica	75°06′00″ S 123°21′00″ E	3233	Ice core	3062.4	δ^{18}O	652000 BC–2000 AD	Jitaru et al., 2009
f4	Dome C	Antarctica	77°39′00″ S 124°10′00″ E	3240	Ice core	905	δ^{18}O	31710 BC–1990 AD	Vandal et al., 1993

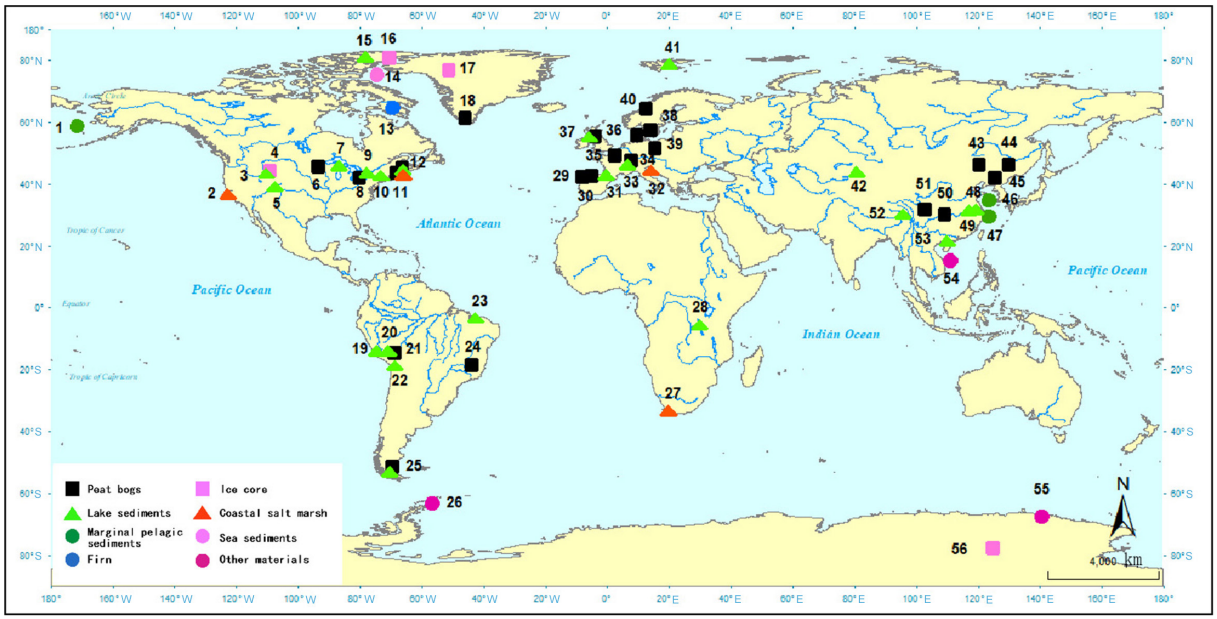

FIGURE 1 | Distribution of mercury deposition research spots. 1. Bering Sea (Kim et al., 2019); 2. San Francisco Bay (Donovan et al., 2013); 3. Wyoming (Kurz et al., 2019); 4. California (Conaway et al., 2004); 5. Colorado (Gray et al., 2005); 6. Minnesota (Benoit et al., 1998); 7. the Great Lakes (Grant et al., 2014); 8. Ontario (Givelet et al., 2004); 9. Lake Ontario (Wiklund et al., 2017); 10. New York (Arnason and Fletcher, 2003); 11. Maine (Roos-Barraclough et al., 2006); 12. the Bay of Fundy (Sunderland et al., 2008); 13. Baffifin Island (Zdanowicz et al., 2015); 14. the Arctic Archipelago (Štrok et al., 2019); 15. Ellesmere Island (Korosi et al., 2018); 16. Arctic Canada (Zdanowicz et al., 2016); 17. northwest Greenland (Zheng, 2015); 18. Narsaq Peninusla (Shotyk et al., 2003); 19. Huancavelica (Cooke et al., 2009); 20. Yanacocha (Beal et al., 2014); 21. Lake Titicaca region (Guédron et al., 2018); 22. Lake Chungará (Guédron et al., 2019); 23. Maranhão state (De Lacerda et al., 2017); 24. Minas Gerais (Peìrez-Rodrìguez et al., 2015); 25. Patagonia (Biester et al., 2002, 2003; Hermanns and Biester, 2013a; Daga et al., 2016); 26. King George Island (Sun et al., 2006); 27. Berg River (Kading et al., 2009); 28. Lake Tanganyika (Conaway et al., 2012); 29. Xistral Mountains (Martínez-Cortizas et al., 2012); 30. Asturias (Gallego et al., 2013); 31. Pyrenees (Corella et al., 2017); 32. Adriatic Sea (Covelli et al., 2012); 33. Lake Lucerne (Thevenon et al., 2011); 34. Swiss Jura Mountains (Roos-Barraclough and Shotyk, 2003); 35. Belgium (Allan et al., 2013); 36. Denmark (Shotyk et al., 2003); 37. Scotland (Farmer et al., 2009; Küttner et al., 2014); 38. Sweden (Bindler et al., 2004); 39. the Czech Republic (Ettler et al., 2008); 40. Norway (Steinnes and Sjøbakk, 2005); 41. Svalbard (Drevnick et al., 2012); 42. Mount Tianshan (Zeng et al., 2014); 43. Greater Khingan Range (Bao et al., 2016); 44. Lesser Khingan Range (Xu, 2010; Tang et al., 2012); 45. Hani peat bog (Xiao, 2017); 46. Yellow Sea (Kim et al., 2019); 47. East China Sea (Lim et al., 2017; Zhang H. X. et al., 2018; Zhang R. et al., 2018); 48. Shanghai (Yang H. D. et al., 2016); 49. Chao Lake (Zhang H. X. et al., 2018; Zhang R. et al., 2018); 50. Dajiu Lake Basin (Li et al., 2016, 2017); 51. Hongyuan (Shi et al., 2011); 52. Tibetan Plateau (Wang et al., 2010; Yang et al., 2010); 53. Huguangyan Maar Lake (Zeng et al., 2017; Han, 2018); 54. Xisha Islands (Xu et al., 2010; Liu et al., 2012); 55. Adélie Basin (Zaferani et al., 2018); and 56. Dome C (Vandal et al., 1993; Jitaru et al., 2009).

and other industrial activities). Due to the interaction between these factors and regional differences in human activities, the mercury deposition changes in different regions showed both certain commonalities and relatively large differences through time. Based on previous studies, the history of global mercury deposition was divided into the following four stages:

670 to 11.7 ka BP, Before the Holocene

The Dome C ice core in Antarctica provided a mercury deposition time series for past 670 ka (**Figure 2**). This record revealed mercury value peaks during glacial periods, while in the warm interglacial periods, the Hg concentration was relatively low (Jitaru et al., 2009). Similar trends occurred in the ice core records of Dome C for the past 34 ka, with greater temporal resolution (**Figure 3A**): The mercury concentration was relatively low 34 ka BP, and then it rose, maintaining a high value during 28 to 18 ka BP, corresponding to the Last Glacial Maximum (LGM, ∼26 to 16 ka BP); there was a reduction in 17 to 13 ka BP, representing the transition from the Last Glacial Period to the Holocene. According to peat records in southeastern Brazil (**Figure 3A**), the mercury concentration fluctuation 57 to 28 ka BP was relatively smooth, and the change in mercury concentration was mainly affected by atmospheric wet deposition related to precipitation and mineral input in the catchment area (Peìrez-Rodrìguez et al., 2015). The mercury concentration suddenly decreased to its lowest value 27 ka BP and then increased sharply and remained high from 26 to 17 ka BP, coinciding with the LGM (**Figure 3A**; Peìrez-Rodrìguez et al., 2015). Similar glacial to interstadial contrast in mercury levels was reported for lake sediment records in northeastern Brazil (De Lacerda et al., 2017). Records from this lake showed decreased Hg concentrations at ca. 17 to 13 ka BP, with subsequent recovery to the level prior to 17 ka BP, and until the sudden increase ca. 12 ka BP, corresponding to the Younger Dryas (YD) cooling event (De Lacerda et al., 2017). The mercury accumulations in the Dajiu Lake Basin, the Swiss Jura Mountains, and Peru also showed a significant increasing trend before and after the YD event (**Figure 3B**). Through the comparison of the above data, we concluded that glacial and interglacial timescales ca. the past 600 ka global mercury deposition appears to fluctuate in parallel

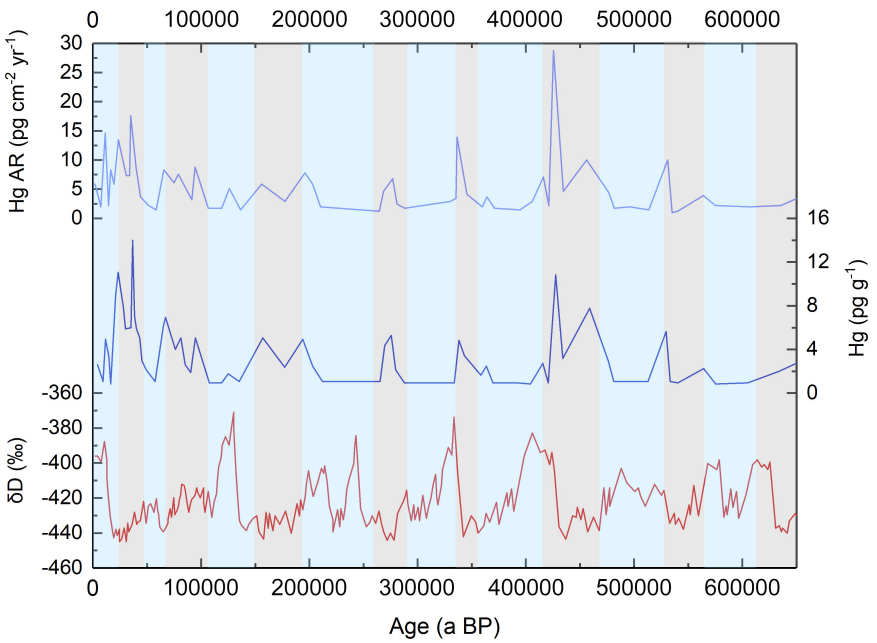

FIGURE 2 | Mercury deposition and temperature change in Antarctica since 670,000 a BP. The data were based on the research results of Petru Jitaru et al. in Dome C ice core of Antarctica, the red curve represents δD (‰), indicating the temperature change (Jitaru et al., 2009).

with broad climate variability with more Hg accumulation in the glacial periods and less accumulation in the interglacial periods.

11.7 to 8.2 ka BP, the Early Holocene

Post YD cooling, in general there was warming in to an interglacial climate. However, in the Early Holocene, the climate was still unstable and there were many climate oscillations sourced in the North Atlantic area, including the 11.1 ka BP event, 10.3 ka BP event, 9.4 ka BP event, 8.2 ka BP event, and possibly other climate variability (Bond et al., 1997). According to the mercury deposition records of the Dajiu Lake Basin, the Swiss Jura Mountains, Lake Titicaca, Yanacocha of Peru, and Maine United States (**Figure 3B**), both the mercury concentration and mercury accumulation rate for the Early Holocene were relatively low and Hg-depositional variability was linked to abrupt changes, especially during the 8.2 ka BP cooling event in the N. Atlantic. The mercury deposition in the Dajiu Lake Basin, the Swiss Jura Mountains, Lake Titicaca, Yanacocha in Peru, and Maine in the United States reached a peak. Through comparison of the regional data, it was discovered that in the Early Holocene, the mercury accumulation rate in the Dajiu Lake Basin of China was higher than that in the Swiss Jura Mountains and Maine in the United States, among other locations. Meanwhile, data from various regions showed that atmospheric mercury deposition was unstable during this period, with substantial fluctuations.

8.2 to 4.2 ka BP, the Mid-Holocene

Many studies showed that the climate in the Mid-Holocene was generally warm and humid (Dwyer et al., 1996; Haug et al., 2001; Kaufman et al., 2004). Global atmospheric mercury deposition was also characterized by relatively consistent values in the Mid-Holocene (**Figures 3B,C**). It is worth noting that the changes in mercury accumulation in some areas during this period were related to specific conditions. For example, the enrichment of mercury deposition from 8 to 6 ka BP in the Swiss Jura Mountains was related to volcanic eruptions (Roos-Barraclough et al., 2002); the mercury peaks of Lake Titicaca from 6 to 5 ka BP were caused by rich orographic precipitation in the eastern part of the Andes (Guédron et al., 2018). The comparison of the regional data showed that in the Mid-Holocene, the characteristics of atmospheric mercury deposition in the Dajiu Lake Basin and Lesser Khingan Range of China, the Swiss Jura Mountains, Spain, Norway, Maine, and Ontario, among other locations, were similar, and the atmospheric mercury accumulation rate and mercury concentrations were at a relatively low level, with the atmospheric mercury deposition being weaker and significantly lower than that during the Early Holocene.

4.2 to 0 ka BP, the Late Holocene

The Late Holocene is a stage when human civilization has developed rapidly and human activities have had a profound impact on natural systems. Since the Industrial Revolution, the population has increased dramatically and the impact of human activities on earth system reached an unprecedented magnitude. Under the multiple effects of natural systems and human activities, regional and global atmospheric mercury deposition changed significantly and the rate of atmospheric mercury accumulation increased to its highest value during historical periods. Atmospheric mercury deposition between 4.2 and 0 ka BP in all regions of the world continued to rise (**Figures 3C,D**), especially in the past hundreds of years. The atmospheric mercury accumulation rate and the mercury

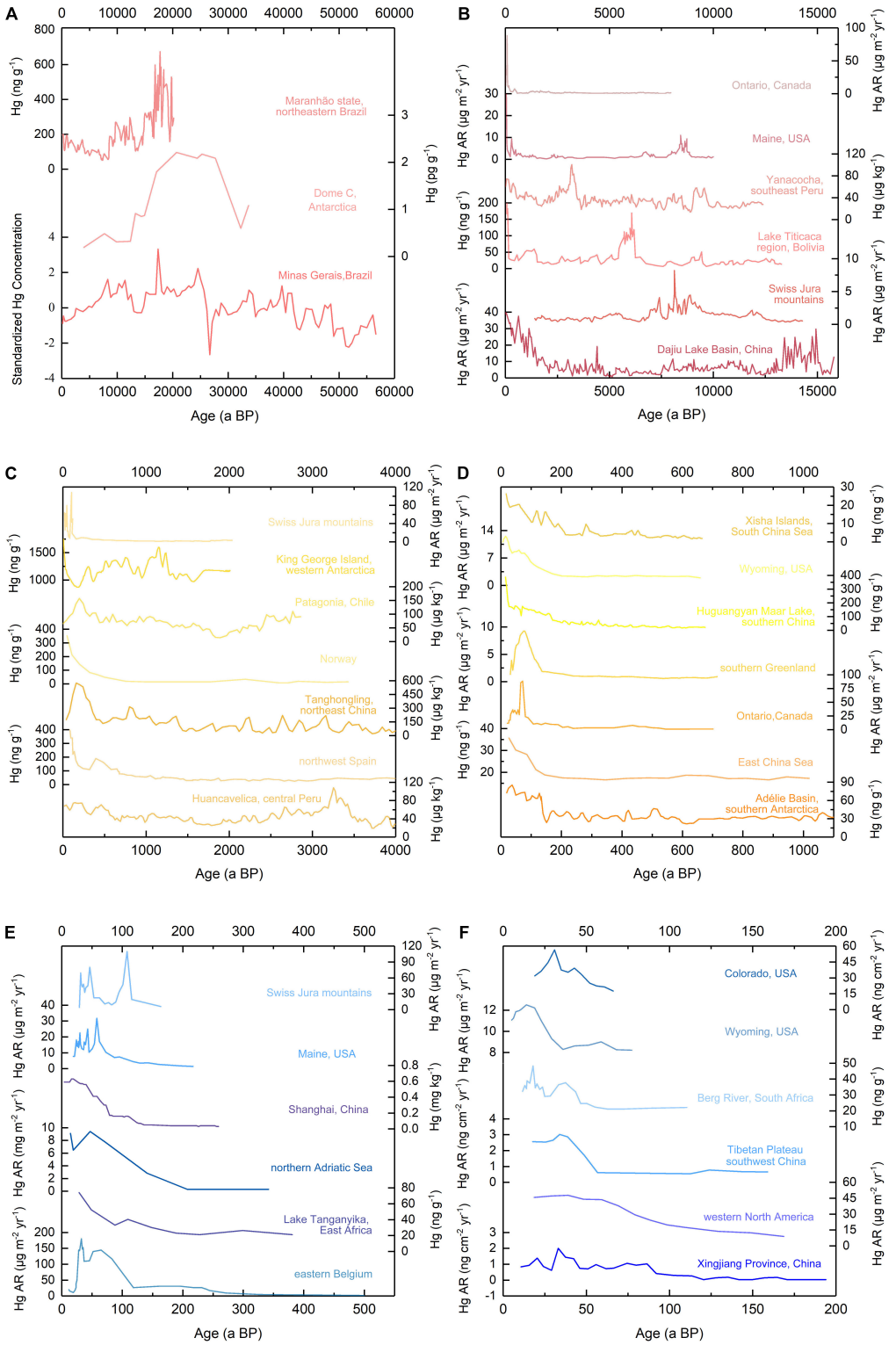

FIGURE 3 | Changes of mercury deposition in different time scales around the world. **(A)** From bottom to top: Standardized Hg concentrations in Minas Gerais, Brazil (Peirez-Rodrîguez et al., 2015); Hg concentrations in Dome C, Antarctica (Vandal et al., 1993); and Hg concentrations in Maranhão state, northeastern Brazil (De Lacerda et al., 2017). **(B)** From bottom to top: Hg Accumulation Rate (Hg AR) in Dajiu Lake Basin, China (Li et al., 2016); Hg AR in Swiss Jura Mountains (Roos-Barraclough et al., 2002); Hg concentrations in Lake Titicaca region, Bolivia (Guédron et al., 2018); Hg concentrations in Yanacocha, southeast Peru (Beal et al., 2014); Hg AR in Maine, United States (Roos-Barraclough et al., 2006); and Hg AR in Ontario, Canada (Givelet et al., 2004). **(C)** From bottom to top: Hg

(Continued)

FIGURE 3 | Continued
concentrations in Huancavelica, central Peru (Beal et al., 2014), northwest Spain (Martínez-Cortizas et al., 1999), Tanghongling, northeast China (Tang et al., 2012), Norway (Steinnes and Sjøbakk, 2005), Patagonia, Chile (Biester et al., 2003), King George Island, western Antarctica (Sun et al., 2006); and Hg AR in Swiss Jura Mountains (Roos-Barraclough et al., 2002). **(D)** From bottom to top: Hg concentrations in Adélie Basin, southern Antarctica (Zaferani et al., 2018), East China Sea (Kim et al., 2019); Hg AR in Ontario, Canada (Givelet et al., 2004), southern Greenland (Pérez-Rodríguez et al., 2017); Hg concentrations in Huguangyan Maar Lake, southern China (Zeng et al., 2017); Hg AR in Wyoming, United States (Kurz et al., 2019); and Hg concentrations in Xisha Islands, South China Sea (Huang et al., 2013). **(E)** From bottom to top: Hg AR in eastern Belgium (Allan et al., 2013); Hg concentrations in Lake Tanganyika, East Africa (Conaway et al., 2012); Hg AR in northern Adriatic Sea (Covelli et al., 2012); Hg concentrations in Shanghai, China (Yang H. D. et al., 2016); and Hg AR in Maine, United States (Roos-Barraclough et al., 2006), Swiss Jura Mountains (Roos-Barraclough et al., 2002). **(F)** From bottom to top: Hg AR in Xingjiang Province, China (Zeng et al., 2014), western North America (Drevnick et al., 2016), Tibetan Plateau, southwest China (Wang et al., 2010); Hg concentrations in Berg River, South Africa (Kading et al., 2009); and Hg AR in Wyoming, United States (Kurz et al., 2019), Colorado, United States (Gray et al., 2005).

concentration reached their highest values during the Mid- and Late Holocene (**Figures 3D,F**). This was mainly due to the significant increase in mercury emissions from human activities after the Industrial Revolution, which led to an increase in the rate of atmospheric mercury accumulation of several times or even tens of times.

Through the comparison of atmospheric mercury deposition data at a global scale, it could be inferred that the characteristics of mercury deposition in European countries represented by Switzerland, Greenland, Spain, and Belgium, among others, are similar to those of the North American countries represented by the United States and Canada. Specifically, beginning with the Industrial Revolution in the mid-19th century, the mercury deposition rate increased rapidly, and mercury accumulation reached a peak value in the mid- and late 20th century and then showed a downward trend. With the increasing emphasis on the environmental pollution caused by a large number of mercury emissions in European and North American countries, measures were taken in various regions to reduce mercury emissions (Roos-Barraclough and Shotyk, 2003; Bindler et al., 2004; Ettler et al., 2008; Sunderland et al., 2008; Farmer et al., 2009; Drevnick et al., 2012; Allan et al., 2013; Corella et al., 2017). The atmospheric mercury deposition rate in the Asian regions represented by Shanghai, the Xisha Islands, Huguangyan Maar Lake, and the East China Sea increased slowly after industrialization. The rate began to increase rapidly during the 1960s to 1970s, with mercury deposition continuing to rise. From the above comparison, it could be deduced that since the 1970s, the center of global mercury production has gradually shifted from Europe and North America to Asia (Xu et al., 2010; Zeng et al., 2017).

Mercury Deposition and Climate Change

In studies around the world, the impact of climate change on mercury deposition has been the focus of researchers with various outcomes. Most scholars believe that a cold and dry climate is conducive to mercury accumulation, while a warm and humid climate limits the accumulation of mercury (Roos-Barraclough et al., 2002, 2006; Jitaru et al., 2009; Gallego et al., 2013; Peìrez-Rodriìguez et al., 2015; Li et al., 2016; De Lacerda et al., 2017). Some scholars believe that there is more mercury accumulation during humid-climate periods and less accumulation of mercury during dry-climate periods (Guédron et al., 2018). Related to this issue, in the following section, two aspects of climate, namely, temperature change and humidity change, are analyzed and summarized.

Dry and Wet Deposition of Atmospheric Mercury

Mercury emitted from anthropogenic and natural sources to the atmosphere eventually falls back to the surface through dry and wet deposition. Dry deposition refers to the deposition of aerosol particles. An aerosol is a gas dispersion composed of solid or liquid particles suspended in a gas medium, which has a complex chemical composition (Wang, 2011). Wet deposition refers to the process of removing particles from the atmosphere through rainfall, snowfall, and other phenomena.

Atmospheric mercury deposition is a process through which various forms of mercury are removed from the atmosphere. The dry deposition of mercury mainly includes the direct deposition of Hg(0) and RGM, which occurs throughout the year as long as it does not rain heavily. The forms of mercury in wet deposition tend to be soluble and granular Hg(II). Due to the long-distance diffusion and water solubility of gaseous Hg(II), most of the mercury is deposited via Hg(II) dissolved in atmospheric water or adsorbed on the surface of raindrop particles (Fitzgerald et al., 1991). Mercury can react with O_3 in the atmosphere to form water-soluble Hg(II), which can be adsorbed on particles or dissolved in water and then deposited. Inorganic mercury compounds, such as methylmercury, deposit rapidly because of their solubility (Munthe et al., 1995). Although the wet deposition process of Hg(II) contributes greatly, it represents less than 5% of the total mercury in the atmosphere, and the continuous dry deposition of mercury almost all year is still dominant. Recent studies employing field monitoring and mercury isotopes showed that Hg(0) dry deposition far exceeds wet deposition by precipitation and the former can even be five times greater than the latter (Selin and Jacob, 2008; Enrico et al., 2016; Obrist et al., 2017; St. Louis et al., 2019).

At present, the deposition mechanism and long-term monitoring sites of mercury wet deposition flux in many countries are well established. As one of the countries emitting the most mercury in the world, China has yet to establish a relatively complete monitoring system for wet mercury deposition. Additionally, the measurement and evaluation of dry mercury deposition are mostly local or achieved by atmospheric models, and there are few published relevant records.

Impact of Temperature Change on Mercury Deposition

To evaluate the impact of temperature change on mercury deposition, the mercury deposition records of Maine of the United States, southeastern Peru, the Swiss Jura Mountains,

Patagonia of Chile, the Shennongjia Dajiu Lake Basin of China, Maranhão of Brazil, Dome C of Antarctica, and Minas Gerais of Brazil were selected for comparison, as shown in **Figure 4**. During the LGM (∼26–16 ka BP), the mercury concentration in Antarctica, as well as Minas Gerais and Maranhao, remained at a high level. From 17 to 13 ka BP, the mercury concentration showed a downward trend until it reached its peak again from 13 to11.5 ka BP, consistent with the YD event, and the mercury accumulation in the Dajiu Lake Basin and Patagonia also showed an obvious upward trend before and after the YD event. From 11.5 to 9 ka BP, the mercury concentration dropped gradually, but the decrease was small, and it increased significantly and reached its peak from 9 to 8 ka BP, corresponding to the 8.2 ka BP event, with the strongest cooling effect during the Holocene.

After 8.2 ka BP, the mercury accumulations generally showed a slow downward trend. The peak values of mercury accumulation in the Mid- and Late Holocene were mainly affected by volcanic eruptions and human activities (Vandal et al., 1993; De Lacerda et al., 2017). Volcanic emissions are thought to be an important natural source of atmospheric Hg. On millennial timescales, dust from volcanic eruptions might affect mercury deposition in paleoclimate records. Hg enrichment in Patagonia occurred during the periods of three volcanic eruptions two eruptions of Mt. Burney (8300 a BP and 4250 a BP) and one eruption of the Mt. Hudson volcano (7800 a BP; **Figure 4D**; Biester et al., 2003). Many volcanoes erupted between 8 and 6 ka BP in Europe, which explained the peaks of the Hg accumulation rate in the Swiss Jura Mountains (**Figure 4C**; Roos-Barraclough et al., 2002).

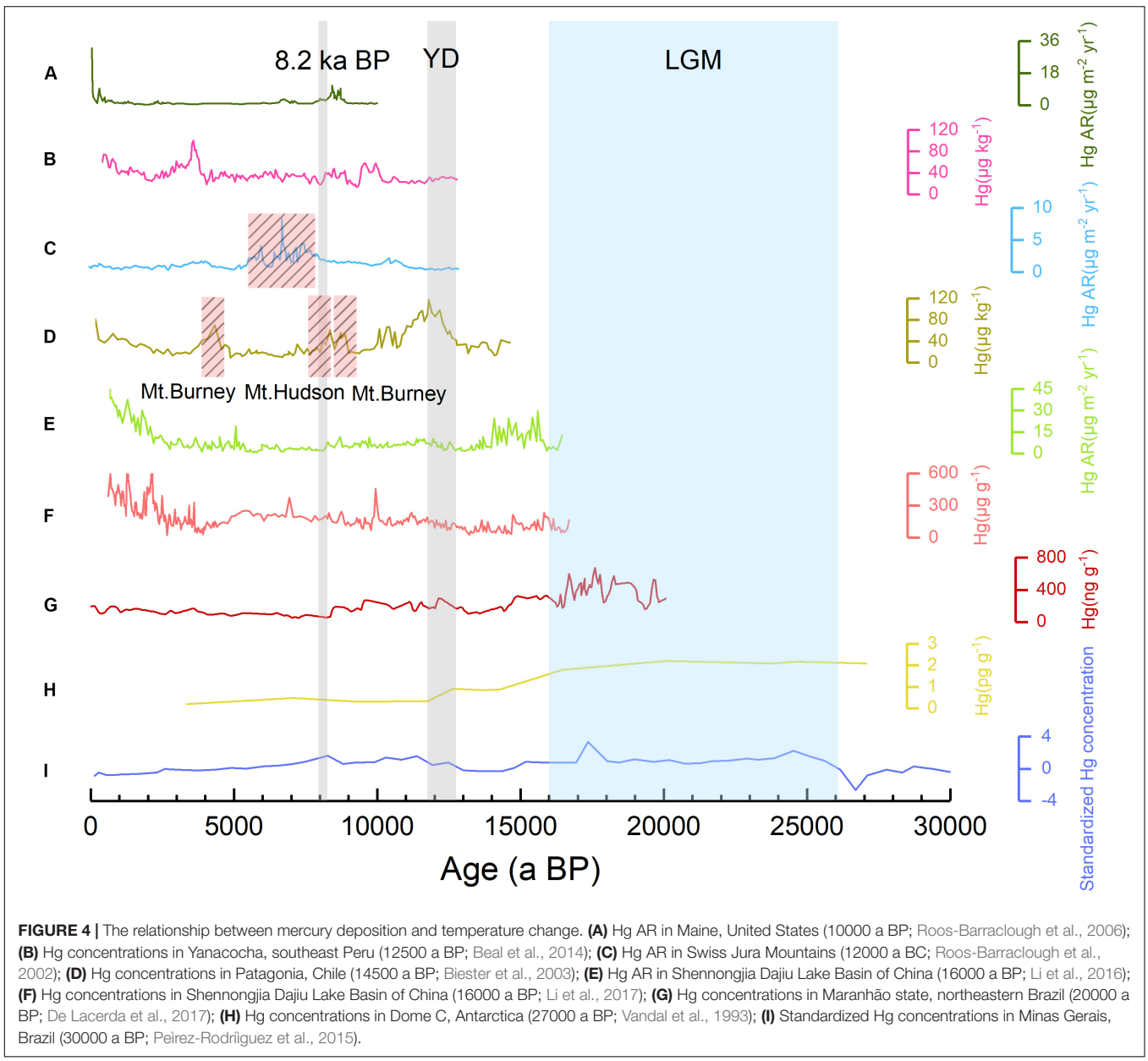

FIGURE 4 | The relationship between mercury deposition and temperature change. **(A)** Hg AR in Maine, United States (10000 a BP; Roos-Barraclough et al., 2006); **(B)** Hg concentrations in Yanacocha, southeast Peru (12500 a BP; Beal et al., 2014); **(C)** Hg AR in Swiss Jura Mountains (12000 a BC; Roos-Barraclough et al., 2002); **(D)** Hg concentrations in Patagonia, Chile (14500 a BP; Biester et al., 2003); **(E)** Hg AR in Shennongjia Dajiu Lake Basin of China (16000 a BP; Li et al., 2016); **(F)** Hg concentrations in Shennongjia Dajiu Lake Basin of China (16000 a BP; Li et al., 2017); **(G)** Hg concentrations in Maranhão state, northeastern Brazil (20000 a BP; De Lacerda et al., 2017); **(H)** Hg concentrations in Dome C, Antarctica (27000 a BP; Vandal et al., 1993); **(I)** Standardized Hg concentrations in Minas Gerais, Brazil (30000 a BP; Peìrez-Rodrìguez et al., 2015).

At longer timescales, it could be concluded that the temperature change from 30 to 8 ka BP was consistent with the fluctuation of atmospheric mercury deposition, especially during the LGM, YD event, and 8.2 ka BP event, and atmospheric mercury deposition showed a strong response. Petru Jitaru et al. reconstructed mercury deposition records and temperature changes since 670 ka BP at Dome C, Antarctica. As shown in **Figure 2**, there is a good correlation between peak mercury accumulation and cold periods. Based on these analyses, it could be concluded that a cold climate is conducive to mercury accumulation. According to the studies of different scholars, the following four reasons could be summarized regarding the specific mechanism: (1) Due to the high volatility of mercury, the mercury in the atmosphere is easily attached to objects such as particulate matter under cold conditions and then settles on the ground surface, known as the condensation effect (Roos-Barraclough et al., 2002; Gallego et al., 2013); (2) The atmospheric dust increases during cold periods, and this dust can carry the mercury in the atmosphere to the ground surface so that mercury accumulation is increased (Roos-Barraclough et al., 2002; Jitaru et al., 2009; Peìrez-Rodriìguez et al., 2015; De Lacerda et al., 2017; Li et al., 2017); (3) In colder environments, marine mercury emissions are higher (Vandal et al., 1993; Roos-Barraclough et al., 2002; Peìrez-Rodriìguez et al., 2015; De Lacerda et al., 2017) and the high-productivity marine emissions of gaseous mercury are important sources of atmospheric mercury (Vandal et al., 1993); and (4)The mercury released by soil degassing is lower during cold periods (Gallego et al., 2013). In conclusion, more exogenous dust inputs and an increase in mercury in the atmosphere during cold periods lead to mercury accumulation on the scale of tens of thousands of years, while on millennial timescales, mercury emitted from volcanic eruption to the atmosphere also has a certain impact on mercury deposition records.

Impact of Humidity Change on Mercury Deposition

The main effect of precipitation on mercury deposition is that an increase in precipitation promotes a rise in forest litterfall Hg deposition. Terrestrial vegetation often represents the first ecosystem compartment with which new atmospheric Hg interacts following deposition. It was recently demonstrated that a portion of newly wet-deposited Hg(II) may not initially pass directly through the forest canopy to the forest floor, but rather is retained over the growing season, only to be deposited later with litterfall (Graydon et al., 2006). Plant foliage provides an excellent surface for photochemical reduction of newly deposited Hg(II) remaining in the forest canopy following precipitation events (Lindberg et al., 1998). Litterfall Hg deposition is the major pathway for Hg loading into the forest (Zhou et al., 2013). Recent studies on the air-surface exchange of mercury and litterfall Hg deposition revealed that an increase in precipitation can elevate forest biomass, which in turn pumps more Hg(0) into litterfall and then soils (Lindberg et al., 1998; Graydon et al., 2006). It is generally believed that vegetation litter represents a net sink of atmospheric Hg (Lindberg et al., 1998; Demers et al., 2007; Pokharel and Obrist, 2011; Ma et al., 2017; Zhang et al., 2019). Therefore, an increase in precipitation may enhance absolute wet Hg deposition rather than wet deposition relative to dry deposition via vegetation. However, research on the mechanism of mercury deposition affected by long-term humidity change is lacking. The results of studies conducted in Brazil and Lake Titicaca showed that the atmospheric wet deposition of mercury during humid periods increased, so a humid climate is considered to be conducive to mercury accumulation (Peìrez-Rodriìguez et al., 2015; Guédron et al., 2018). However, most scholars found a significant relationship between a cold-dry climate and peak mercury deposition. Unfortunately, the influence of temperature could not be excluded to judge the relationships between humidity changes and mercury deposition. Furthermore, due to the small amount of data and conclusions available for reference, the relationship between humidity change and mercury deposition cannot be determined. The authors believe that studies of the relationship between precipitation changes and mercury deposition changes can be strengthened over long timescales and a more accurate conclusion can be drawn by comparing the two types of change.

Mercury Deposition and Anthropogenic Activities

According to a large number of previous studies, atmospheric mercury deposition caused by human activities began approximately 3,500 years ago. Before industrialization, gold, silver, and mercury mining and the widespread use of cinnabar were the main sources of anthropogenic mercury. After industrialization, coal combustion, mercury mining, non-ferrous metal smelting, liquid mercury production, steel manufacturing, cement manufacturing, gold mining, waste incineration, and the development of the chlor-alkali industry led to a sharp increase in anthropogenic emissions of mercury, which in turn caused a sharp increase in mercury deposition.

Preindustrial Era

With the development of human civilization, mercury is being increasingly used in all aspects of society. Cinnabar has a bright red color and never fades, so it has long been used as a pigment. According to the literature, the use of cinnabar can be traced back to the Shang Dynasty (∼1600–1046 BC) in China, and some characters engraved with cinnabar were found on unearthed animal bones or turtle shells (Li et al., 2016). Cinnabar was also used to color figurines and pottery; for example, the Terracotta Warriors were painted with cinnabar (Chen, 2017). In ancient times, mercury was considered an antiseptic, and mercury gas volatilized in underground palaces could prevent buried corpses and funerary objects from rotting for a long time. Since mercury is a highly toxic substance that can cause death in cases of inhalation at high volume, it was also used to poison tomb raiders (Liu and Wang, 2001; Duan, 2007). During the Qin and Han Dynasties of China (221 BC–220 AD), Chinese ancestors extracted elemental mercury from cinnabar, utilizing the easy solubility of gold and silver in mercury and the volatility of mercury to extract gold and silver from ores by using mercury, which was later called the "amalgamation process" (Li et al., 2016). For quite a long time in ancient times, the amalgamation process was the main method of gold smelting worldwide, until it was replaced by a more effective method with less mercury

pollution called the "cyanidation method" in the early 20th century (Sun et al., 2006). Mercury was also used in medicine. According to the manuscripts on silk named "Prescriptions for Fifty-two Diseases" in the Han Dynasty Changsha Mawangdui Tomb unearthed in 1973, transcription was performed during the Qin and Han Dynasties. It was the most ancient Chinese medicine prescription that has been discovered, in which mercury was used in four prescriptions. Moreover, mercury was once considered by Tibetans to be able to heal fractures, prolong life, and maintain good health (Wang et al., 2010; Yang et al., 2010).

At approximately 1400 BC, the Huancavelica cinnabar mine in Peru began to be mined. During the period of rapid development and expansion of mining and metallurgy in the Andes (∼500–1000 AD, ∼1000–1400 AD), mercury emissions increased continuously (Cooke et al., 2009). In Europe, the increase in anthropogenic mercury 2500 years ago was consistent with the high mercury mining activities and metallurgical history of Spain (Martínez-Cortizas et al., 1999). **Figure 5** shows that the mercury concentrations in various regions were higher in some stages between 2000 years ago and the beginning of industrialization, namely, the Roman Empire (27 BC–1453 AD), the Chinese Han Dynasty (202 BC–8 AD, 25–220 AD), the Mayan period (from approximately the 10th century BC to the 16th century AD), the Chinese Tang Dynasty (618–907 AD), and after the discovery of the New World (1650–1800 AD). The high mercury concentrations were closely related to the large-scale mining activities during these periods. However, between these periods, with the decrease in mining activities, the mercury concentrations showed a downward trend. Between 18 and 300 AD, both the Roman Empire and the Chinese Han Dynasty engaged in many mining activities when alchemy became popular at the time (Martínez-Cortizas et al., 1999; Sun et al., 2006). After 300 AD, the mercury concentrations declined. Between 300 and 750 AD, the mercury concentrations were relatively low, corresponding to the collapse of Rome and the decline in China's gold production (Brading and Cross, 1972; Sun et al., 2006). Between 1050 and 1250 AD, low mercury concentrations corresponded to the fall of Mayan civilization and the wars during the Southern Song Dynasty. In addition, the depletion of European silver mines and the suppression of gold mining also led to a decrease in mercury concentration (Sun et al., 2006). Since the beginning of 1250 AD, the mercury concentrations have increased, and during the period of Incan civilization in South America (from the 12th to 15th century), a large amount of gold was produced (Xiang and Huang, 2014). Meanwhile, new silver mines were discovered in Europe, and thousands of people joined the "Silver Tide" activities of the Christian Kingdom (Sun et al., 2006). After 1500 AD, the mercury concentrations fell to another low. Pizarro, a Spanish colonist, conquered the Inca in 1532 AD (Xiang and Huang, 2014), resulting in a reduction in mercury consumption. In the early 19th century, with the outbreak of the South American War of Independence, mercury consumption suddenly stopped and Spain, the main supplier of mercury in the world, also reduced mercury production (Martínez-Cortizas et al., 1999), leading to a decline in mercury concentration. With the rise of the Industrial Revolution in the mid-19th century, mercury concentrations began to rise sharply.

Industrial Age

Since the Industrial Revolution of 1840, coal combustion, non-ferrous metal smelting, and the chlor-alkali industry have become the main sources of anthropogenic mercury. Intensive industrial activities have caused unprecedented mercury pollution. According to previous studies, in Spain, the mercury accumulation after industrialization was 10 times as high as the level before industrialization (Serrano et al., 2013). In Norway, the figure was 15 (Steinnes and Sjøbakk, 2005); in Scotland, the figure was 20 (Farmer et al., 2009); and in Belgium, the figure was 63 (Allan et al., 2013). After the 1960s and 1970s, since European and North American countries began to pay attention to environmental issues and adopted a series of measures to reduce mercury emissions, such as closing the main mercury mines, reducing mercury emissions from flue gas emissions, reducing incinerator emissions, gradually phasing out mercury in waste streams, shutting down old facilities, and installing additional pollution control equipment (Benoit et al., 1998; Conaway et al., 2004; Sunderland et al., 2008; Yang H. D. et al., 2016; Yang J. et al., 2016; Corella et al., 2017; Obrist et al., 2018), mercury deposition was reduced to some extent. However, after the 1970s, with the rise of Asian countries, especially China and India, and the rapid development of industrialization and urbanization, Asia became the largest contributor to anthropogenic mercury, with its mercury emission accounting for more than half of the global emission in 2000 (Xu et al., 2010; Obrist et al., 2018). In recent decades, the massive production of mercury in Asia, coupled with the high mercury emissions from coal combustion, smelting, and waste incineration, has led to a significant increase in anthropogenic mercury emissions (Liu et al., 2012). This means that the mercury production center has gradually moved from Europe and North America to Asia.

Factors Influencing Mercury Deposition in Different Phases or at Different Timescales

Based on the previous analysis, it could be concluded that the main factors influencing mercury deposition include temperature change, human activities, and volcanic eruption, while the influencing factors vary among phases and timescales. According to **Figures 2**, **4**, before the Middle and Late Holocene, when human activities had limited environmental impact, mercury deposition was consistent with temperature changes. That is, on the scale of hundreds of thousands of years, mercury accumulated more in cold periods and less in warm periods, and mercury mainly came from exogenous dust inputs. On millennial timescales, the correspondence between mercury deposition and temperature change shows limited significance, while the former is more closely related to volcanic eruption and human activities (**Figures 4**, **5**; Vandal et al., 1993; De Lacerda et al., 2017). The frequent volcanic eruptions in the Middle Holocene led to the peak of mercury accumulation in this period (Roos-Barraclough et al., 2002). With the change in human activities in the past 3,500 years, mercury deposition has shown strong correspondence.

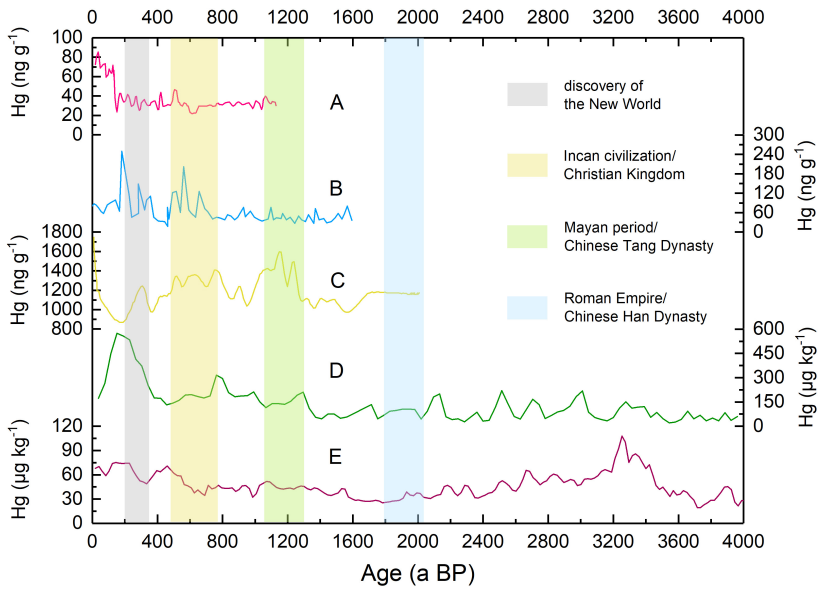

FIGURE 5 | Relationship between mercury deposition and human activities since 4000 a BP. **(A)** Hg concentrations in Adélie Basin, southern Antarctica (1100 a BP; Zaferani et al., 2018); **(B)** Hg concentrations in Patagonia, Chile (1600 a BP; Daga et al., 2016); **(C)** Hg concentrations in King George Island, western Antarctica (2000 a BP; Sun et al., 2006); **(D)** Hg concentrations in Lesser Khingan Range (4000 a BP; Tang et al., 2012); and **(E)** Hg concentrations in Huancavelica, central Peru (4000 a BP; Beal et al., 2014).

SUMMARY AND PROSPECTS

Summary

This study summarized the characteristics of mercury deposition from a global perspective by analyzing previous studies on mercury deposition on yearly to 100,000-year timescales. It was found that regarding the accumulation of mercury, there are certain commonalities within the regional range, while there are also differences among regions. In addition, both climate change and human activities have a significant impact on mercury deposition.

(1) The common feature of global mercury deposition in the Holocene is that the accumulation was generally lower before the start of the Industrial Revolution of 1840 and posthaste increased rapidly. Alternatively, due to regional volcanic activities or human activities, such as mining and metallurgy, there are differences in mercury accumulations among regions. It is worth noting that since the 1970s, emission reduction measures have been adopted in Europe and North America to reduce mercury accumulation, and Asia has gradually become the global center of anthropogenic mercury emissions.

(2) On the scale of hundreds of thousands of years, mercury accumulated more in cold periods and less in warm periods. On millennial timescales, the correspondence between mercury deposition and temperature change appears non-significant, and the former is more closely related to volcanic eruption and human activities. An increase in precipitation leads to a rise in forest litterfall Hg deposition. Little research has been performed on the effect of long-term humidity change on mercury deposition, with inconsistent conclusions, so the specific impact of humidity change on mercury deposition is unknown.

(3) The atmospheric mercury deposition caused by human activities can be traced back to 3500 years ago. Before industrialization, gold, silver, and mercury mining and the widespread use of cinnabar were the main anthropogenic mercury sources; after industrialization, coal combustion, non-ferrous metal smelting, waste incineration, and chlor-alkali industry development led to a significant increase in anthropogenic emissions of mercury, which in turn led to a sharp increase in mercury deposition.

Prospects

Although many studies have been conducted on the relationships of mercury deposition with climate change and human activities, with significant results, there remains some urgent challenges from a global perspective.

(1) The mercury deposition monitoring and research sites are unevenly distributed. The research sites are mostly distributed in the Northern Hemisphere, including Western Europe, North America, and China, while the number of research areas distributed in the Southern Hemisphere is relatively small, located in only a few regions of South America, Africa, and Antarctica. There are no research sites in Eastern Europe, Northern and Central Asia, Northern Africa, or Oceania. In future studies, mercury deposition research in these gap areas can be strengthened to provide data for the global reconstruction of the evolutionary history of mercury deposition.

(2) Most previous studies focused on the history of mercury deposition in the Holocene. There have been few studies on a longer timescale and even fewer studies on the relationship between precipitation change and mercury accumulation. As a result, the impact of climate change, especially humidity change, on the mercury accumulation mechanism has yet to be investigated. Therefore, it is suggested that studies of mercury deposition on a longer timescale and of the impact of precipitation on mercury accumulation be strengthened.
(3) There is a lack of high-resolution mercury deposition reconstruction. In previous studies, fen peat and lacustrine deposits were widely used as natural archives, with few ice core records with high resolution and almost no stalagmite records available. To accurately analyze the relationships of mercury deposition with climate change and human activities, mercury deposition reconstruction at a higher resolution should be performed.

AUTHOR CONTRIBUTIONS

FL and CM designed the research. FL presented a synthesis of the state of the art of mercury deposition worldwide. FL and PZ completed the data collection, analysis, and interpretation. All authors listed have made substantial, direct and intellectual contributions to the work, and approved it for publication. All authors contributed to the article and approved the submitted version.

FUNDING

This research was jointly funded by the National Natural Science Foundation of China (Nos. 41671196 and 41977389) and the National Key Research and Development Program of China (No. 2016YFA0600501).

ACKNOWLEDGMENTS

We are grateful to Renhui Huang and Chujun Yuan for their valuable suggestions about the final version of the manuscript. We also acknowledge Yunkai Deng and Haiyan Li for their assistance with the graphics. Our deepest gratitude goes to the two reviewers and the Associate Editor Liangcheng Tan as well as the Chief Editor Steven L. Forman for their careful work and thoughtful suggestions which have helped improve this manuscript substantially.

REFERENCES

Allan, M., Le Roux, G., Sonke, J. E., Piotrowska, N., Streel, M., and Fagel, N. (2013). Reconstructing historical atmospheric mercury deposition in Western Europe using: Misten peat bog cores, Belgium. *Sci. Total Environ.* 442, 290–301. doi: 10.1016/j.scitotenv.2012.10.044

Arnason, J. G., and Fletcher, B. A. (2003). A 40+ year record of Cd, Hg, Pb, and U deposition in sediments of Patroon Reservoir, Albany County, NY, USA. *Environ. Pollut.* 123, 383–391. doi: 10.1016/S0269-7491(03)00015-0

Bao, K., Shen, J., Wang, G., Sapkota, A., and McLaughlin, N. (2016). Estimates of recent Hg pollution in Northeast China using peat profiles from Great Hinggan Mountains. *Environ. Earth Sci.* 75:536. doi: 10.1007/s12665-015-5231-8

Beal, S. A., Kelly, M. A., Stroup, J. S., Jackson, B. P., Lowell, T. V., and Tapia, P. M. (2014). Natural and anthropogenic variations in atmospheric mercury deposition during the Holocene near Quelccaya Ice Cap, Peru. *Global Biogeochem. Cycles* 28, 437–450. doi: 10.1002/2013GB004780

Benoit, J. M., Fitzgerald, W. F., and Damman, A. W. H. (1998). The biogeochemistry of an ombrotrophic bog: evaluation of use as an archive of atmospheric mercury deposition. *Environ. Res.* 78, 118–133. doi: 10.1006/enrs.1998.3850

Biester, H., Bindler, R., Martinez-Cortizas, A., and Engstrom, D. R. (2007). Modeling the past atmospheric deposition of mercury using natural archives. *Environ. Sci. Technol.* 41, 4851–4860. doi: 10.1021/es0704232

Biester, H., Kilian, R., Franzen, C., Woda, C., Mangini, A., and SchÖler, H. F. (2002). Elevated mercury accumulation in a peat bog of the Magellanic Moorlands, Chile (53°S) – an anthropogenic signal from the Southern Hemisphere. *Earth Planet. Sci. Lett.* 201, 609–620. doi: 10.1016/S0012-821X(02)00734-3

Biester, H., Martinez-Cortizas, A., Birkenstock, S., and Kilian, R. (2003). Effect of peat decomposition and mass loss on historic mercury records in peat bogs from patagonia. *Environ. Sci. Technol.* 37, 32–39. doi: 10.1021/es025657u

Bindler, R., Klarqvist, M., Klaminder, J., and Förster, J. (2004). Does within-bog spatial variability of mercury and lead constrain reconstructions of absolute deposition rates from single peat records? The example of Store Mosse, Sweden. *Global Biogeochem. Cycles* 18:GB3020. doi: 10.1029/2004gb002270

Bond, G., Showers, W., Cheseby, M., Lotti, R., Almasi, P., De Menocal, P., et al. (1997). A pervasive millennial-scale cycle in North Atlantic Holocene and Glacial Climates. *Science* 278, 1257–1266. doi: 10.1126/science.278.5341.1257

Brading, D. A., and Cross, H. E. (1972). Colonial silver mining: Mexico and Peru. *Hisp. Am. Hist. Rev.* 52, 545–579. doi: 10.2307/2512781

Chen, G. Y. (2017). Cinnabar mercury industry in the Qin Empire. *J. Shaanxi Norm. Univ.* 46, 71–81.

Conaway, C. H., Swarzenski, P. W., and Cohen, A. S. (2012). Recent paleorecords document rising mercury contamination in Lake Tanganyika. *Appl. Geochem.* 27, 352–359. doi: 10.1016/j.apgeochem.2011.11.005

Conaway, C. H., Watson, E. B., Flanders, J. R., and Flegal, A. R. (2004). Mercury deposition in a tidal marsh of South San Francisco Bay downstream of the historic New Almaden mining district, California. *Mar. Chem.* 90, 175–184. doi: 10.1016/j.marchem.2004.02.023

Cooke, C. A., Balcom, P. H., Biester, H., and Wolfe, A. P. (2009). Over three millennia of mercury pollution in the Peruvian Andes. *Proc. Natl. Acad. Sci. U.S.A.* 106, 8830–8834. doi: 10.1073/pnas.0900517106

Corella, J. P., Valero-Garcés, B. L., Wang, F., Martínez-Cortizas, A., Cuevas, C. A., and Saiz-Lopez, A. (2017). 700 years reconstruction of mercury and lead atmospheric deposition in the Pyrenees (NE Spain). *Atmos. Environ.* 155, 97–107. doi: 10.1016/j.atmosenv.2017.02.018

Covelli, S., Langone, L., Acquavita, A., Piani, R., and Emili, A. (2012). Historical flux of mercury associated with mining and industrial sources in the Maranoand Grado Lagoon (Northern Adriatic Sea). *Estuar. Coast. Shelf Sci.* 113, 7–19. doi: 10.1016/j.ecss.2011.12.038

Daga, R., Ribeiro Guevara, S., Pavlin, M., Rizzo, A., Lojen, S., Vreèa, P., et al. (2016). Historical records of mercury in southern latitudes over 1600 years: lake Futalaufquen. Northern Patagonia. *Sci. Total Environ.* 553, 541–550. doi: 10.1016/j.scitotenv.2016.02.114

De Lacerda, L. D., Turcq, B., Sifeddine, A., and Cordeiro, R. C. (2017). Mercury accumulation rates in Caço Lake, NE Brazil during the past 20,000 years. *J. S. Am. Earth Sci.* 77, 42–50. doi: 10.1016/j.jsames.2017.04.008

Demers, J. D., Driscoll, C. T., Fahey, T. J., and Yavitt, J. B. (2007). Mercury cycling in litter and soil in different forest types in the Adirondack region, New York, USA. *Ecol. Appl.* 17, 1341–1351. doi: 10.1890/06-1697.1

Donovan, P. M., Blum, J. D., Yee, D., and Gehrke, G. E. (2013). An isotopic record of mercury in San Francisco Bay sediment. *Chem. Geol.* 349-350, 87–98. doi: 10.1016/j.chemgeo.2013.04.017

Drevnick, P. E., Cooke, C. A., Barraza, D., Blais, J. M., Coale, K. H., Cumming, B. F., et al. (2016). Spatiotemporal patterns of mercury accumulation in lake sediments of western North America. *Sci. Total Environ.* 568, 1157–1170. doi: 10.1016/j.scitotenv.2016.03.167

Drevnick, P. E., Yang, H., Lamborg, C. H., and Rose, N. L. (2012). Net atmospheric mercury deposition to Svalbard: estimates from lacustrine sediments. *Atmos. Environ.* 59, 509–513. doi: 10.1016/j.atmosenv.2012.05.048

Duan, Q. B. (2007). *Research on the Related Problems of the Mausoleum of the First Emperor of Qin Dynasty*. Kirkland, WA: Northwest University.

Dwyer, T. R., Mullins, H. T., and Good, S. C. (1996). Paleoclimatic implications of Holocene lake-level fluctuations, Owasco Lake, New York. *Geology* 24, 519–522.

Enrico, M., Roux, G. L., Marusczak, N., Heimbürger, L. E., Claustres, A., Fu, X. W., et al. (2016). Atmospheric mercury transfer to peat bogs dominated by gaseous elemental mercury dry deposition. *Environ. Sci. Technol.* 50, 2405–2412. doi: 10.1021/acs.est.5b06058

Ettler, V., Navrátil, T., Mihaljevič, M., Rohovec, J., Zuna, M., Šebek, O., et al. (2008). Mercury deposition/accumulation rates in the vicinity of a lead smelter as recorded by a peat deposit. *Atmos. Environ.* 42, 5968–5977. doi: 10.1016/j.atmosenv.2008.03.047

Farmer, J. G., Anderson, P., Cloy, J. M., Graham, M. C., Mackenzie, A. B., and Cook, G. T. (2009). Historical accumulation rates of mercury in four Scottish ombrotrophic peat bogs over the past 2000 years. *Sci. Total Environ.* 407, 5578–5588. doi: 10.1016/j.scitotenv.2009.06.014

Fitzgerald, W. F., Mason, R. P., and Vandal, G. M. (1991). Atmosphere cycling and air-water exchange of Hg over mid-continental Lacustrine regions. *Water Air Soil Pollut.* 56, 745–767. doi: 10.1007/bf00342314

Gallego, J. L. R., Ortiz, J. E., Sierra, C., Torres, T., and Llamas, J. F. (2013). Multivariate study of trace element distribution in the geological record of Roñanzas Peat Bog (Asturias, N. Spain). Paleoenvironmental evolution and human activities over the last 8000 cal yr BP. *Sci. Total Environ.* 454-455, 16–29. doi: 10.1016/j.scitotenv.2013.02.083

Givelet, N., Roos-Barraclough, F., and Shotyk, W. (2004). Predominant anthropogenic sources and rates of atmospheric mercury accumulation in southern Ontario recorded by peat cores from three bogs: comparison with natural "background" values past 8000 years. *J. Environ. Monit.* 5, 935–949. doi: 10.1039/B307140E

Grant, S. L., Kim, M., Lin, P., Crist, K. C., Ghosh, S., and Kotamarthi, V. R. (2014). A simulation study of atmospheric mercury and its deposition in the Great Lakes. *Atmos. Environ.* 94, 164–172. doi: 10.1039/B307140E

Gray, J. E., Fey, D. L., Holmes, C. W., and Lasorsa, B. K. (2005). Historical deposition and fluxes of mercury in Narraguinnep Reservoir, southwestern Colorado. USA. *Appl. Geochem.* 20, 207–220. doi: 10.1016/j.apgeochem.2004.05.011

Graydon, J. A., St. Louis, V. L., Lindberg, S. E., Hintelmann, H., and Krabbenhoft, D. P. (2006). Investigation of mercury exchange between forest canopy vegetation and the atmosphere using a new dynamic chamber. *Environ. Sci. Technol.* 40, 4680–4688. doi: 10.1021/es0604616

Guédron, S., Ledru, M. P., Escobar-Torrez, K., Develle, A. L., and Brisset, E. (2018). Enhanced mercury deposition by Amazonian orographic precipitation: evidence from high-elevation Holocene records of the Lake Titicaca region (Bolivia). *Palaeogeogr. Palaeoclimat. Palaeoecol.* 511, 577–587. doi: 10.1016/j.palaeo.2018.09.023

Guédron, S., Tolu, J., Brisset, E., Sabatier, P., Perrot, V., Bouchet, S., et al. (2019). Late Holocene volcanic and anthropogenic mercury deposition in the western Central Andes (Lake Chungará, Chile). *Sci. Total Environ.* 662, 903–914. doi: 10.1016/j.scitotenv.2019.01.294

Han, C. (2018). *The History of Atmospheric Mercury Deposition Since 1200 Years Recorded in the Sediments of Huguangyan Maar Lake, Zhanjiang*. Beijing: China University of Geosciences.

Haug, G. H., Hughen, K. A., Sigman, D. M., Peterson, L. C., and Röhl, U. (2001). Southward migration of the intertropical convergence zone through the Holocene. *Science* 293, 1304–1308. doi: 10.1126/science.1059725

Hermanns, Y. M., and Biester, H. (2013a). A 17,300-year record of mercury accumulation in a pristine lake in southern Chile. *J. Paleolimnol.* 49, 547–561. doi: 10.1007/s10933-012-9668-4

Hermanns, Y. M., and Biester, H. (2013b). Anthropogenic mercury signals in lake sediments from southernmost Patagonia, Chile. *Sci. Total Environ.* 445-446, 126–135. doi: 10.1016/j.scitotenv.2012.12.034

Huang, J., Kang, S. C., Zhang, Q. G., and Guo, J. M. (2013). "Study on atmospheric mercury wet deposition in the Tibet Plateau and its adjacent areas. Environmental Chemistry Committee of Chinese Chemical Society, Environmental Chemistry Branch of Chinese Society of Environmental Science," in *Summary of the 7th National Conference on Environmental Chemistry-S12 Heavy metal pollution and remediation. Environmental Chemistry Committee of Chinese Chemical Society, Environmental Chemistry Branch of Chinese Society of Environmental Science*.

Jitaru, P., Gabrielli, P., Marteel, A., Plane, J. M. C., Planchon, F. A. M., Gauchard, P. A., et al. (2009). Atmospheric depletion of mercury over Antarctica during glacial periods. *Nat. Geosci.* 2, 505–508. doi: 10.1038/ngeo549

Kading, T. J., Mason, R. P., and Leaner, J. J. (2009). Mercury contamination history of an estuarine floodplain reconstructed from a 210Pb-dated sediment core (Berg River, South Africa). *Mar. Pollut. Bull.* 59, 116–122. doi: 10.1016/j.marpolbul.2009.02.020

Kaufman, D. S., Ager, T. A., Anderson, N. J., Anderson, P. M., Andrews, J. T., Bartlein, P. T., et al. (2004). Erratum to: holocene thermal maximum in the western Arctic (0-180°W). *Quat. Sci. Rev.* 23, 529–560. doi: 10.1016/j.quascirev.2003.09.007

Kim, H., Lee, K., Lim, D., Nam, S., Han, S. H., Kim, J., et al. (2019). Increase in anthropogenic mercury in marginal sea sediments of the Northwest Pacific Ocean. *Sci. Total Environ.* 654, 801–810. doi: 10.1016/j.scitotenv.2018.11.076

Korosi, J. B., Griffiths, K., Smol, J. P., and Blais, J. M. (2018). Trends in historical mercury deposition inferred from lake sediment cores across a climate gradient in the Canadian High Arctic. *Environ. Pollut.* 241, 459–467. doi: 10.1016/j.envpol.2018.05.049

Krabbenhoft, D. P., and Sunderland, E. M. (2013). Global change and mercury. *Environ. Sci.* 341, 1457–1458. doi: 10.1126/science.1242838

Kurz, A. Y., Blum, J. D., Washburn, S. J., and Baskaran, M. (2019). Changes in the mercury isotopic composition of sediments from a remote alpine lake in Wyoming, USA. *Sci. Total Environ.* 669, 973–982. doi: 10.1016/j.scitotenv.2019.03.165

Küttner, A., Mighall, T. M., De Vleeschouwer, F., Maukuoy, D., Martínez-Cortizas, A., Foster, I. D. L., et al. (2014). A 3300-year atmospheric metal contamination record from Raeburn Flow raised bog, south west Scotland. *J. Archaeol. Sci.* 44, 1–11. doi: 10.1016/j.jas.2014.01.011

Li, Y. P., Ma, C. M., Zhu, C., Huang, R., and Zheng, C. G. (2016). Historical anthropogenic contributions to mercury accumulation recorded by a peat core from Dajiuhu montane mire, central China. *Environ. Pollut.* 216, 332–339. doi: 10.1016/j.envpol.2016.05.083

Li, Y. P., Ma, C. M., Zhu, C., Huang, R., and Zheng, C. G. (2017). Hg sedimentary records and influencing factors of Dajiuhu Lake Basin since 16,000 years ago. *China Environ. Sci.* 37, 1103–1110.

Lim, D., Kim, J., Xu, Z. K., Jeong, K., and Jung, H. (2017). New evidence for Kuroshio inflow and deepwater circulation in the Okinawa Trough, East China Sea: sedimentary mercury variations over the last 20 kyr. *Paleoceanography* 32, 571–579. doi: 10.1002/2017PA003116

Lindberg, S. E., Hanson, P. J., Meyers, T. P., and Kim, K. H. (1998). Air/surface exchange of mercury vapor over forests—the need for a reassessment of continental biogenic emissions. *Atmos. Environ.* 32, 895–908. doi: 10.1016/S1352-2310(97)00173-8

Liu, C. H., and Wang, Z. Y. (2001). From the view of "Taking mercury as rivers and seas", the antiseptic measures in the tombs of the Eastern Zhou, Qin and Han Dynasties in China. *Collect. Comment. Qin Cult.* 42, 1–439.

Liu, X. D., Xu, L. Q., Chen, Q. Q., Sun, L. G., Wang, Y. H., Yan, H., et al. (2012). Historical change of mercury pollution in remote Yongle archipelago, South China Sea. *Chemosphere* 87, 549–556. doi: 10.1016/j.chemosphere.2011.12.065

Ma, M., Du, H. X., Wang, D. Y., Sun, T., Sun, S. W., and Yang, G. (2017). The fate of mercury and its relationship with carbon, nitrogen and bacterial communities during litter decomposing in two subtropical forests. *Appl. Geochem.* 86, 26–35. doi: 10.1016/j.apgeochem.2017.09.008

Martínez-Cortizas, A., Peiteado Varela, E., Bindle, R., Biester, H., and Cheburkin, A. (2012). Reconstructing historical Pb and Hg pollution in NW Spain using multiple cores from the Chao de Lamoso bog (Xistral Mountains). *Geochim. Cosmochim. Acta* 82, 68–78. doi: 10.1016/j.gca.2010.12.025

Martínez-Cortizas, A., Pontevedra-Pombal, X., Garcı a-Rodeja, E., Nóvoa-Muñoz, C., and Shotyk, W. (1999). Mercury in a Spanish peat bog: archive of climate change and atmospheric metal deposition. *Science* 284, 939–942. doi: 10.1126/science.284.5416.939

Megaritis, A. G., Murphy, B. N., Racherla, P. N., Adams, P. J., and Pandis, S. N. (2014). Impact of climate change on mercury concentrations and deposition in the eastern United States. *Sci. Total Environ.* 487, 299–312. doi: 10.1016/j.scitotenv.2014.03.084

Munthe, J., Hultberg, H., Lee, Y. H., Parkman, H., Iverfeldt, A., and Renberg, I. (1995). Trends of mercury and methyl-mercury in deposition, run-off water sediments in relation to experimental manipulations and acidification. *Water Air Soil Pollut.* 85, 743–748. doi: 10.1007/BF00476918

Obrist, D., Agnan, Y., Jiskra, M., Olson, C. L., Colegrove, D. P., Hueber, J., et al. (2017). Tundra uptake of atmospheric elemental mercury drives Arctic mercury pollution. *Nature* 547, 201–204. doi: 10.1038/nature22997

Obrist, D., Kirk, J. L., Zhang, L., Sunderland, E. M., Jiskra, M., and Selin, N. E. (2018). A review of global environmental mercury processes in response to human and natural perturbations: changes of emissions, climate, and land use. *Ambio* 47, 116–140. doi: 10.1007/s13280-017-1004-9

Pérez-Rodríguez, M., Silva-Sánchez, N., Kylander, M. E., Bindler, R., Mighall, T. M., Edward Schofield, J., et al. (2017). Industrial-era lead and mercury contamination in southern Greenland implicates North American sources. *Sci. Total Environ.* 613–614, 919–930. doi: 10.1016/j.scitotenv.2017.09.041

Peirez-Rodriıguez, M., Horaik-Terra, I., Rodriıguez-Lado, L., Aboal, J. R., and Martínez-Cortizas, A. (2015). Long-term (˜57 ka) controls on mercury accumulation in the Southern Hemisphere reconstructed using a peat record from Pinheiro Mire (Minas Gerais, Brazil). *Environ. Sci. Technol.* 49, 1356–1364. doi: 10.1021/es504826d

Pokharel, A. K., and Obrist, D. (2011). Fate of mercury in tree litter during decomposition. *Biogeosciences* 8, 2507–2521. doi: 10.5194/bg-8-2507-2011

Pratte, S., Bao, K., Shen, J., Mackenzie, L., Klamt, A. M., Wang, G. P., et al. (2018). Recent atmospheric metal deposition in peatlands of northeast China: a review. *Sci. Total Environ.* 626, 1284–1294. doi: 10.1016/j.scitotenv.2018.01.183

Roos-Barraclough, F., Givelet, N., Cheburkin, A. K., Shotyk, W., and Norton, S. A. (2006). Use of Br and Se in peat to reconstruct the natural and anthropogenic fluxes of atmospheric Hg: a 10000-year record from Caribou Bog, Maine. *Environ. Sci. Technol.* 40, 3188–3194. doi: 10.1021/es051945p

Roos-Barraclough, F., Martínez-Cortizas, A., García-Rodeja, E., and Shotyk, W. (2002). A 14 500 year record of the accumulation of atmospheric mercury in peat: volcanic signals, anthropogenic influences and a correlation to bromine accumulation. *Earth Planet. Sci. Lett.* 202, 435–451. doi: 10.1016/S0012-821X(02)00805-1

Roos-Barraclough, F., and Shotyk, W. (2003). Millennial-scale records of atmospheric mercury deposition obtained from ombrotrophic and minerotrophic peatlands in the Swiss Jura Mountains. *Environ. Sci. Technol.* 37, 235–244. doi: 10.1021/es0201496

Schuster, P. F., Krabbenhoft, D. P., Naftz, D. L., Dewayne Cecil, L., Olson, M. L., Dewild, J. F., et al. (2002). Atmospheric mercury deposition during the last 270 years: a glacial ice core record of natural and anthropogenic sources. *Environ. Sci. Technol.* 36, 2303–2310. doi: 10.1021/es0157503

Selin, N. E., and Jacob, D. J. (2008). Seasonal and spatial patterns of mercury wet deposition in the United States: constraints on the contribution from North American anthropogenic sources. *Atmos. Environ.* 42, 5193–5204. doi: 10.1016/j.atmosenv.2008.02.069

Serrano, O., Martínez-Cortizas, A., Mateo, M. A., Biester, H., and Bindler, R. (2013). Millennial scale impact on the marine biogeochemical cycle of mercury from early mining on the Iberian Peninsula. *Global Biogeochem. Cycles* 27, 21–30. doi: 10.1029/2012GB004296

Shi, W. F., Feng, X. B., Zhang, G., Ming, L. L., Yin, R. S., Zhao, Z. Q., et al. (2011). High resolution mercury isotope records in rain fed peat of Hongyuan in the past 150 years. *Chin. Sci. Bull.* 56, 583–588.

Shotyk, W., Goodsite, M. E., Roos-barraclough, F., Frei, R., Heinemeier, J., Asmund, G., et al. (2003). Anthropogenic contributions to atmospheric Hg, Pb and As accumulation recorded by peat cores from southern Greenland and Denmark dated using the 14C "bomb pulse curve". *Geochim. Cosmochim. Acta* 67, 3991–4011. doi: 10.1016/S0016-7037(03)00409-5

St. Louis, V. L., Graydon, J. A., Lehnherr, I., Amos, H. M., Sunderland, E. M., St. Pierre, K. A., et al. (2019). Atmospheric concentrations and wet/dry loadings of mercury at the remote experimental lakes area, Northwestern Ontario, Canada. *Environ. Sci. Technol.* 53, 8017–8026. doi: 10.1021/acs.est.9b01338

Steinnes, E., and Sjøbakk, T. E. (2005). Order-of-magnitude increase of Hg in Norwegian peat profiles since the outset of industrial activity in Europe. *Environ. Pollut.* 137, 365–370. doi: 10.1016/j.envpol.2004.10.008

Štrok, M., Anabelle Baya, P., Dietrich, D., Dimock, B., and Hintelmann, H. (2019). Mercury speciation and mercury stable isotope composition in sediments from the Canadian Arctic Archipelago. *Sci. Total Environ.* 671, 655–665. doi: 10.1016/j.scitotenv.2019.03.424

Sun, L. G., Yin, X. B., Liu, X. D., Zhu, R. B., Xie, Z. Q., and Wang, Y. H. (2006). A 2000-year record of mercury and ancient civilizations in seal hairs from King George Island, West Antarctica. *Sci. Total Environ.* 368, 236–247. doi: 10.1016/j.scitotenv.2005.09.092

Sunderland, E. M., Cohen, M. D., Selin, N. E., and Chmura, G. L. (2008). Reconciling models and measurements to assess trends in atmospheric mercury deposition. *Environ. Pollut.* 156, 526–535. doi: 10.1016/j.envpol.2008.01.021

Tang, S. L., Huang, Z. W., Liu, J., Yang, Z. C., and Lin, Q. H. (2012). Atmospheric mercury deposition recorded in an ombrotrophic peat core from Xiaoxing'an Mountain, Northeast China. *Environ. Res.* 118, 145–148. doi: 10.1016/j.envres.2011.12.009

Thevenon, F., Guédron, S., Chiaradia, M., Loizeau, J. L., and Poté, J. (2011). (Pre-) historic changes in natural and anthropogenic heavy metals deposition inferred from two contrasting Swiss Alpine lakes. *Quat. Sci. Rev.* 30, 224–233. doi: 10.1016/j.quascirev.2010.10.013

Vandal, G. M., Fitzgerald, W. F., Boutron, C. F., and Candelone, J. P. (1993). Variations in mercury deposition to Antarctica over the past 34,000 years. *Nature* 362, 621–623. doi: 10.1038/362621a0

Wang, X. P., Yang, H. D., Gong, P., Zhao, X., Wu, G. J., Turner, S., et al. (2010). One century sedimentary records of polycyclic aromatic hydrocarbons, mercury and trace elements in the Qinghai Lake, Tibetan Plateau. *Environ. Pollut.* 158, 3065–3070. doi: 10.1016/j.envpol.2010.06.034

Wang, Y. M. (2011). *Study on Mercury and its Precipitation in the Main Urban Area of Chongqing*. Chongqing: Southwest University, doi: 10.7666/d.y1881755

Wiklund, J. A., Kirk, J. L., Muir, D. C. G., Evans, M., Yang, F., Keating, J., et al. (2017). Anthropogenic mercury deposition in Flin Flon Manitoba and the Experimental Lakes Area Ontario (Canada): a multi-lake sediment core reconstruction. *Sci. Total Environ.* 586, 685–695. doi: 10.1016/j.scitotenv.2017.02.046

Xiang, Y., and Huang, Z. F. (2014). The characteristics and influence of Spanish American colonial rule in the 15th-18th Century. *J. Qiongzhou Univ.* 21, 96–102. doi: 10.13307/j.issn.1008-6722.2014.06.16

Xiao, H. (2017). *Study of Holocene Climate Change and Atmospheric Mercury Deposition Recorded by Peat in Northeast China*. Wuhan: China University of Geosciences.

Xu, J. M. (2010). *Response Relationship between Atmospheric Mercury Deposition and Climate Change Recorded by Rain Fed Peat in Tanghongling, Xiaoxing'anling*. Jiaozuo: Henan Polytechnic University.

Xu, L. Q., Liu, X. D., Sun, L. G., Chen, Q. Q., Yan, H., Liu, Y., et al. (2010). A 700-year record of mercury in avian eggshells of Guangjin Island, South China Sea. *Environ. Pollut.* 159, 889–896. doi: 10.1016/j.envpol.2010.12.021

Yang, H. D., Battarbee, R. W., Turner, S., Rose, N. L., Derwent, R. G., Wu, G. J., et al. (2010). Historical reconstruction of mercury pollution across the Tibetan Plateau using lake sediments. *Environ. Sci. Technol.* 44, 2918–2924. doi: 10.1021/es9030408

Yang, H. D., Turner, S., and Rose, N. L. (2016). Mercury pollution in the lake sediments and catchment soils of anthropogenically-disturbed sites across England. *Environ. Pollut.* 219, 1092–1101. doi: 10.1016/j.envpol.2016.09.012

Yang, J., Chen, L., Steele, J. C., Chen, R. S., and Meng, X. Z. (2016). An extended study on historical mercury accumulation in lake sediment of Shanghai: the contribution of socioeconomic driver. *Environ. Pollut.* 219, 612–619. doi: 10.1016/j.envpol.2016.06.028

Zaccone, C., Santoro, A., Cocozza, C., Terzano, R., Shotyk, W., and Miano, T. M. (2008). Comparison of Hg concentrations in ombrotrophic peat and corresponding humic acids, and implications for the use of bogs as archives of atmospheric Hg deposition. *Geoderma* 148, 399–404. doi: 10.1016/j.geoderma.2008.11.017

Zaferani, S., Pérez-Rodríguez, M., and Biester, H. (2018). Diatom ooze-A large marine mercury sink. *Science* 361, 797–800. doi: 10.1126/science.aat2735

Zdanowicz, C. M., Kruemmel, E., Lean, D., Poulain, A., Kinnard, C., Yumvihoze, E., et al. (2015). Pre-industrial and recent (1970–2010) atmospheric deposition of sulfate and mercury in snow on southern Baffin Island, Arctic Canada. *Sci. Total Environ.* 509-510, 104–114. doi: 10.1016/j.scitotenv.2014.04.092

Zdanowicz, C. M., Krümmel, E. M., Poulain, A. J., Yumvihoze, E., Chen, J. B., Štrok, M., et al. (2016). Historical variations of mercury stable isotope ratios in Arctic glacier firn and ice cores. *Global Biogeochem. Cycles* 30, 1324–1347. doi: 10.1002/2016GB005411

Zeng, H. A., Wu, J. L., and Liu, W. (2014). Two-century sedimentary record of heavy metal pollution from Lake Sayram: a deep mountain lake in central Tianshan, China. *Quat. Int.* 321, 125–131. doi: 10.1016/j.quaint.2013.09.047

Zeng, Y., Chen, J. G., Yang, Y. Q., Wang, J. X., Zhu, Z. J., and Li, J. (2017). Huguangyan Maar Lake (SE China): a solid record of atmospheric mercury pollution history in a non-remote region. *J. Asian Earth Sci.* 147, 1–8. doi: 10.1016/j.jseaes.2017.07.009

Zhang, H., Nizzetto, L., Feng, X. B., Borgå, K., Sommar, J., Fu, X. W., et al. (2019). Assessing air-surface exchange and fate of mercury in a subtropical forest using a novel passive exchange-meter device. *Environ. Sci. Technol.* 53, 4869–4879. doi: 10.1021/acs.est.8b06343

Zhang, H. X., Huo, S. L., Yeager, K. M., Xi, B. D., Zhang, J. T., and Wu, F. C. (2018). A historical sedimentary record of mercury in a shallow Eutrophic Lake: impacts of human activities and climate change. *Engineering* 5, 296–304. doi: 10.1016/j.eng.2018.11.022

Zhang, R., Russell, J., Xiao, X., Zhang, F., Li, T. G., Liu, Z. Y., et al. (2018). Historical records, distributions and sources of mercury and zinc in sediments of East China Sea: implication from stable isotopic compositions. *Chemosphere* 205, 698–708. doi: 10.1016/j.chemosphere.2018.04.100

Zheng, J. C. (2015). Archives of total mercury reconstructed with ice and snow from Greenland and the Canadian High Arctic. *Sci. Total Environ.* 509-510, 133–144. doi: 10.1016/j.scitotenv.2014.05.078

Zhou, J., Feng, X. B., Liu, H. Y., Zhang, H., Fu, X. W., Bao, Z. D., et al. (2013). Examination of total mercury inputs by precipitation and litterfall in a remote upland forest of Southwestern China. *Atmos. Environ.* 81, 364–372. doi: 10.1016/j.atmosenv.2013.09.010

Conflict of Interest: The authors declare that the research was conducted in the absence of any commercial or financial relationships that could be construed as a potential conflict of interest.